Supporting Information

$Au^{\delta-}-O_v-Ti^{3+}$ Interfacial Site: Catalytic Active Center toward Low-Temperature Water Gas Shift Reaction

Ning Liu,[1#] Ming Xu,[2#] Yusen Yang,[1] Shaomin Zhang,[1] Jian Zhang,[1] Wenlong Wang,[1] Lirong Zheng,*[3] Song Hong,*[1] Min Wei*[1]

[1] *State Key Laboratory of Chemical Resource Engineering, Beijing Advanced Innovation Center for Soft Matter Science and Engineering, Beijing University of Chemical Technology, Beijing 100029, People's Republic of China*

[2] *College of Chemistry and Molecular Engineering and College of Engineering, BIC-ESAT, Peking University, Beijing 100871, People's Republic of China*

[3] *Institute of High Energy Physics, the Chinese Academy of Sciences, Beijing 100049, People's Republic of China*

[*] Corresponding authors. Tel: +86-10-64412131; Fax: +86-10-64425385.

E-mail addresses: zhenglr@ihep.ac.cn (L. Zheng); hongsong@mail.buct.edu.cn (S. Hong); weimin@mail.buct.edu.cn (M. Wei).

Experimental section

1. CO chemisorption experiments. CO chemisorption was carried out in a quartz tube reactor on an Automated Catalyst Characterization System (AutoChem 2920) equipped with an on-line mass spectrometry (MS). For the three reduced samples, prior to measurement, 100 mg of sample was firstly pretreated at 200 ℃, 300 ℃, 400 ℃ in H_2 atmosphere for 1 h, respectively, followed by purging with high purity He for 1.0 h; and then the temperature was decreased to 200 K. Afterwards, CO was introduced with He as carrier gas, until the CO MS signal kept stable. The determined dispersion of Au (D_r%) was obtained based on the following equation:

$$D_\mathrm{r}(\%) = \frac{SF \times V_\mathrm{ad} \times M_\mathrm{Au}}{m_\mathrm{s} \times W_\mathrm{s} \times V_\mathrm{m}} \times 100 \qquad (1)$$

The theoretical dispersion of Au (D_t %) was calculated according to Au particle size based on TEM and an assumed spherical model:

$$D_\mathrm{t}(\%) = \frac{6 \times N_s \times M_\mathrm{Au}}{N_\mathrm{A} \times D_\mathrm{Au} \times \rho_\mathrm{Au}} \times 100 \qquad (2)$$

The coverage degree of Au nanoparticle (θ) was calculated based on the following equation:

$$\theta(\%) = (1 - \frac{D_\mathrm{r}}{D_\mathrm{t}}) \times 100 \qquad (3)$$

The surface concentration of Au species n_s (mmol g^{-1}) was calculated by the following equation:

$$n_\mathrm{s} = \frac{W_\mathrm{s} \times D_\mathrm{t}}{M_\mathrm{Au}} \qquad (4)$$

Where SF is the stoichiometric factor, which is assumed as 1:1 for CO:Au at 200 K; V_ad is the volume of chemisorption CO; M_Au is the molecular weight of Au (196.97 g mol^{-1}); m_s is the weight of sample (0.1 g); W_s is the weight fraction of Au; V_m is the molar volume of CO at the standard state (22.4 L); N_s is the number of Au atoms at the surface per unit area (1.15×10^{19} m^{-2}); N_A is the Avogadro's number (6.02×10^{23} mol^{-1}); D_{Au} is the average particle size of Au determined by TEM; ρ_{Au} is the density of metal Au (19.5 g cm^{-3}).

2. EPR characterization. The electron paramagnetic resonance (EPR) spectra were performed on a Bruker E500 spectrometer with 9.53 GHz X-band. Before detection, 5 mg of sample was placed inside a quartz tube (4 mm O.D.), followed by evacuation at room temperature until the residual pressure below 10^{-3} Torr. Finally, the sample was installed in Dewar flasks with temperature decreased to 100 K.

3. XAS characterization. *In situ* extended X-ray absorption fine structure spectroscopy (EXAFS) at the Au L_3-edge and Ti *K*-edge was carried out at the beamline 1W1B of the Beijing Synchrotron Radiation Facility (BSRF), Institute of High Energy Physics (IHEP), Chinese Academy of Sciences (CAS). The typical energy of the storage ring was 2.5 GeV with a maximum current of 250 mA. The Si (111) double crystal monochromator was used. The powdered sample was first pressed into a thin round sheet with a diameter of 13 cm and placed into an *in situ* reaction cell equipped with polyimide windows. The detailed experiment procedure is described as follows:

(1) *In situ* EXAFS spectra at Au L_3-edge: Due to partial overlapping of Au L_3-edge by Zn *K*-edge, the loading of Au was adjusted from 2% to 15% (determined: 13.8 wt.%) to obtain a good signal-to-noise (S/N) ratio for Au absorption spectroscopy. After a reduction treatment in a 5 volume % H_2/He stream at 200 ℃, 300 ℃, and 400 ℃ for 2 h at a heating rate of 5 ℃ min^{-1}, respectively, a high purity He flushing (50 mL min^{-1}) was introduced and slowly cooled to 25 ℃.

Finally, EXAFS spectra at the Au L_3-edge were collected.

(2) *In situ* EXAFS spectra at Au L_3-edge with introduction of reagent: The catalyst was firstly reduced in a 5 volume % H_2/He stream at 300 ℃ for 2 h at a heating rate of 5 ℃ min^{-1}, followed by flowing a high purity He (50 mL min^{-1}) and cooling to 250 ℃, and then EXAFS spectra at Au L_3-edge were collected. Subsequently, H_2O vapor was introduced into the *in situ* reaction cell *via* a HPLC pump, and Au L_3-edge EXAFS spectra were collected within 30 min. Finally, a switch to 5 volume % CO/He atmosphere was performed for the collection of Au L_3-edge EXAFS spectra for another 30 min.

(3) *Operando* EXAFS spectra at Au L_3-edge: The sample was firstly reduced in a 5 volume % H_2/He stream at 300 ℃ for 2 h at a heating rate of 5 ℃ min^{-1}, followed by flowing a high purity He (50 mL min^{-1}) and cooling to 250 ℃, and then EXAFS spectra at Au L_3-edge were collected. Subsequently, a mixture of CO, H_2O and He (6% CO, 25% H_2O and 69% He) was introduced into the reactor with a total flux of 100 ml min^{-1}, and then Au L_3-edge EXAFS spectra were collected under stable *operando* conditions at 250 ℃ for 30 min.

(4) *In situ* EXAFS spectra at Ti *K*-edge: Before detection, the samples were reduced in a 5 volume % H_2/He stream at 200 ℃, 300 ℃, and 400 ℃ for 2 h at a heating rate of 5 ℃ min^{-1}, respectively, then cooled to 25 ℃ in a high purity He flushing (50 mL min^{-1}) for the measurement of Ti *K*-edge EXAFS spectra.

(5) *In situ* EXAFS spectra at Ti *K*-edge with introduction of reagent: The catalyst was firstly reduced in a 5 volume % H_2/He stream at 300 ℃ for 2 h at a heating rate of 5 ℃ min^{-1}, followed by flowing a high purity He (50 mL min^{-1}) and cooling to 250 ℃, and then EXAFS spectra at Ti

K-edge were collected. Subsequently, H_2O vapor was introduced into the *in situ* reaction cell *via* a HPLC pump, and Ti *K*-edge EXAFS spectra were collected within 30 min. Finally, a switch to 5 volume % CO/He atmosphere was performed for the collection of Ti *K*-edge EXAFS spectra for another 30 min.

(6) *Operando* EXAFS spectra at Ti *K*-edge: The sample was firstly reduced in a 5 volume % H_2/He stream at 300 ℃ for 2 h at a heating rate of 5 ℃ min^{-1}, followed by flowing a high purity He (50 mL min^{-1}) and cooling to 250 ℃, and then EXAFS spectra at Ti *K*-edge were collected. Subsequently, a mixture of CO, H_2O and He (6% CO, 25% H_2O and 69% He) was introduced into the reactor with a total flux of 100 ml min^{-1}, and then Ti *K*-edge EXAFS spectra were collected under stable *operando* conditions at 250 ℃ for 30 min.

4. *Quasi in situ* XPS experiments. *Quasi in situ* X-ray photoelectron spectra (XPS) were obtained on an AXIS SUPRA X-ray photoelectron spectrometer operated at a pressure of 2×10^{-9} Torr, using monochromatized Al Kα radiation (1486.6 eV) with a beam diameter of 100 μm. Before exploration, the sample was first pre-reduced in a micro quartz tube reactor, and was painted onto a conductive tape in a vacuum glove box. Finally, the sample was transferred to XPS instrument by using a transport chamber, strictly avoiding air during the whole process.

5. *In situ* DRIFTS experiments. *In situ* diffuse reflectance Fourier transform infrared spectroscopy (*in situ* DRIFTS) was carried out in an *in situ* reaction cell on a Bruker TENSOR II spectrometer equipped with a MCT narrow-band detector. The detailed pre-treatment and test conditions are given as follows:

(1) *In situ* DRIFTS spectra for various samples at 25 ℃: Before CO adsorption, 20 mg of sample

was loaded into the *in situ* reaction cell, pre-treatment in a flow stream of 5 volume % H_2/He (35 ml min^{-1}) at different temperatures (200, 300, 400 ℃) for 2 h with a heating rate of 5 ℃ min^{-1} and then cooled to 25 ℃. The gas flow was switched to high purity He to collect background spectrum. Subsequently, a mixture gas of 5 volume % CO/He (35 ml min^{-1}) was introduced into the cell, and then DRIFTS spectra were collected until the CO adsorption signals kept unchanged.

(2) *In situ* DRIFTS spectra for Au@TiO_{2-x}/ZnO(H300) and Au@ZnO/TiO_2(O300) at various temperatures: For the Au@TiO_{2-x}/ZnO(H300) sample, prior to CO adsorption, 20 mg of sample was loaded into the *in situ* reaction cell, pre-treatment in a flow stream of 5 volume % H_2/He (35 ml min^{-1}) at 300 ℃ for 2 h with a heating rate of 5 ℃ min^{-1} and then cooled to 25 ℃. The gas flow was switched to high purity He to collect background spectrum. After that, CO was introduced into the cell, and CO adsorption signals were collected at different temperatures varying from 25 ℃ to 300 ℃. For the Au@ZnO/TiO_2(O300) sample, it was loaded into the *in situ* reaction cell without pre-treatment, and then CO adsorption signals were collected at temperatures varying from 25 ℃ to 300 ℃.

6. Catalytic evaluations. A continuous flow fixed-bed with a quartz reactor (8 mm I.D.) was used for catalytic evaluations at atmospheric pressure and a temperature range from 125 ℃ to 325 ℃, equipped with an online GC-2014C Shimadzu gas chromatograph. Prior to evaluation, for the reduced samples, 0.5 g of catalyst was pretreated in a mixture gas of 40 volume % H_2/N_2 (100 ml min^{-1}) at 200 ℃, 300 ℃, 400 ℃ for 2 h, respectively (the temperature ramping rate was 5 ℃ min^{-1}), following by cooling to 125 ℃ in high purity N_2 stream. For the reference sample, a calcination in air at 300 ℃ for 2 h was performed. After the pre-treatment, the catalyst was exposed to the mixed gas (CO: 6%, H_2O: 25%, Ar: 69%), water was introduced into the system by a HPLC pump and mixed with CO in a vaporizer maintained at 150 ℃. The measurements were performed at a total gas flow of 110 mL min^{-1}, using a fixed amount of diluted catalysts (0.5 g) to ensure the weight hourly space velocity (WHSV) maintained at 13200 mL $\mathrm{g_{cat}}^{-1}$ h^{-1}. The evaluation was carried out within temperature range from 125 ℃ to 325 ℃, keeping reaction at each temperature for 2 h. Influent and effluent gases were analyzed by online gas chromatography with a TDX-01column and TCD detector. Ar internal standard method was used to determine the composition of the outlet gas. The coefficients of CO and CO_2 were determined using standard samples. In the quantification, CO conversion was calculated based on the following formula:

$$X_{CO}=\frac{[CO_2]_{out}}{[CO_2]_{out}+[CO]_{out}} \qquad (5)$$

In order to calculate TOF value and reaction rate, the CO conversion was kept below 15%. The TOF value and reaction rate were defined as:

$$\mathrm{TOF}=\frac{\text{Mol of CO converted}}{\text{mol of metallic Au surface atom}\times \text{time(s)}} \qquad (6)$$

$$\text{reaction rate}=\frac{\text{Mol of CO converted}}{\text{mol of metallic Au}\times \text{time(s)}} \qquad (7)$$

Stability evaluation was performed under the same reaction conditions as catalytic evaluation. After pre-treatment, the catalyst was exposed to the reformate gas at 300 ℃ for 60 h. Start/stop cycles test was carried out 5 cycles. During each cycle the reaction temperature was raised to 300 ℃ and maintained for 1 h to evaluate catalytic performance, and then cooled to room temperature and kept for another 1 h.

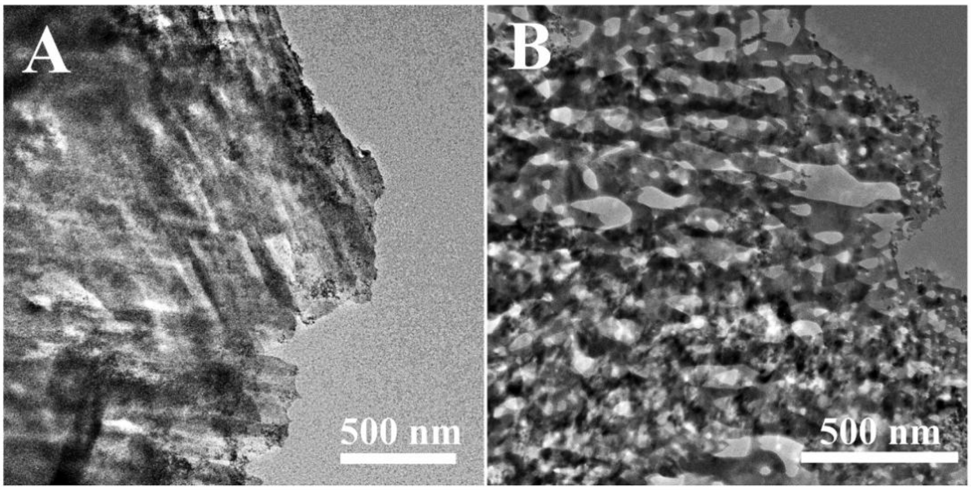

Figure S1. TEM images of (A) ZnTi-LDHs, (B) ZnTi-MMO.

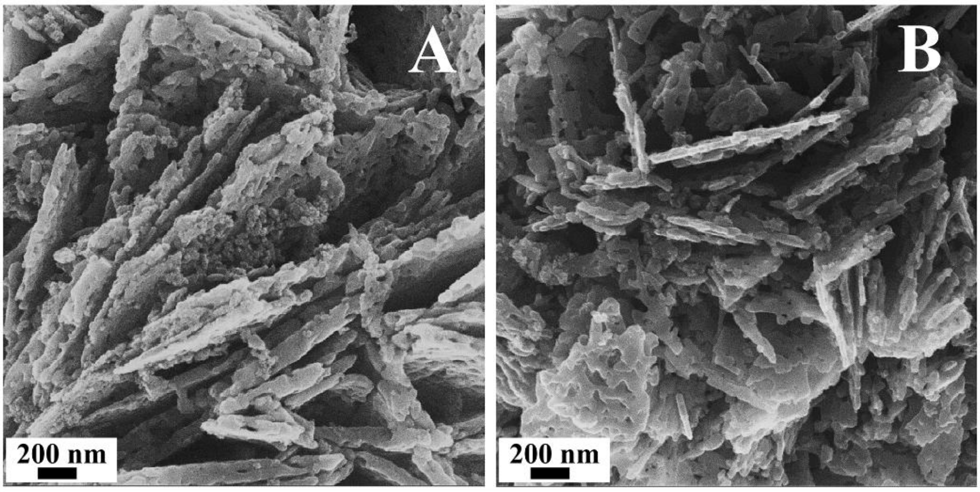

Figure S2. SEM images of (A) Au@TiO_{2-x}/ZnO(H200), (B) Au@TiO_{2-x}/ZnO(H400).

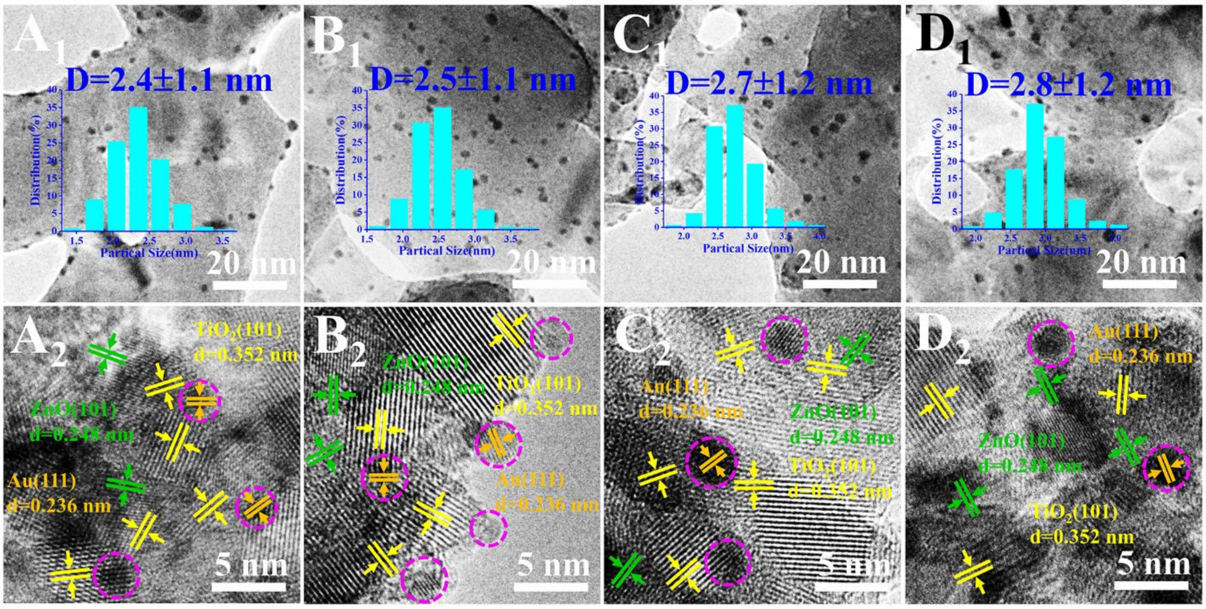

Figure S3. TEM and HRTEM images of (A) Au@TiO_{2-x}/ZnO(H200), (B) Au@TiO_{2-x}/ZnO(H300), (C) Au@TiO_{2-x}/ZnO(H400), (D) Au@ZnO/TiO_2(O300). The size distributions were obtained by analyzing about 200 Au NPs from TEM images.

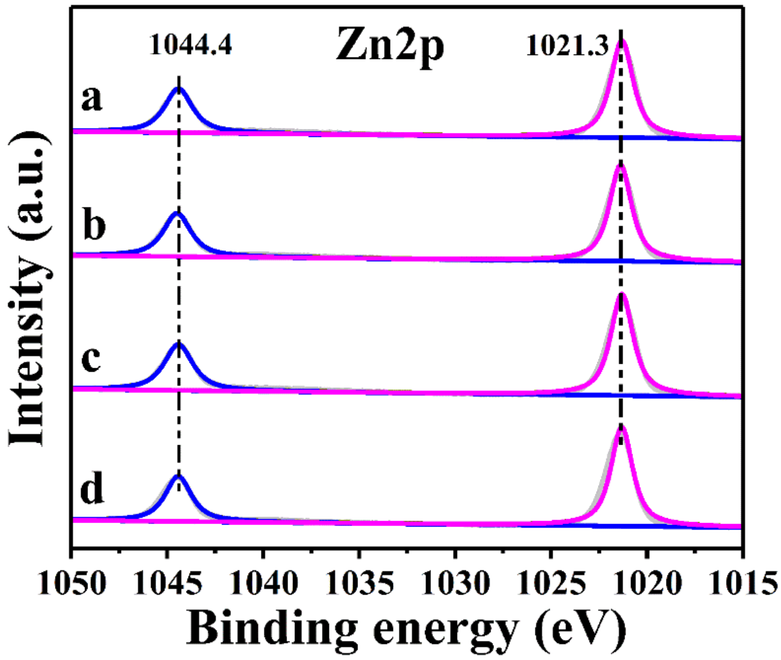

Figure S4. XPS spectra of Zn 2*p* for: (a) Au@TiO_{2-x}/ZnO(H200), (b) Au@TiO_{2-x}/ZnO(H300), (c) Au@TiO_{2-x}/ZnO(H400), (d) Au@ZnO/TiO_2(O300).

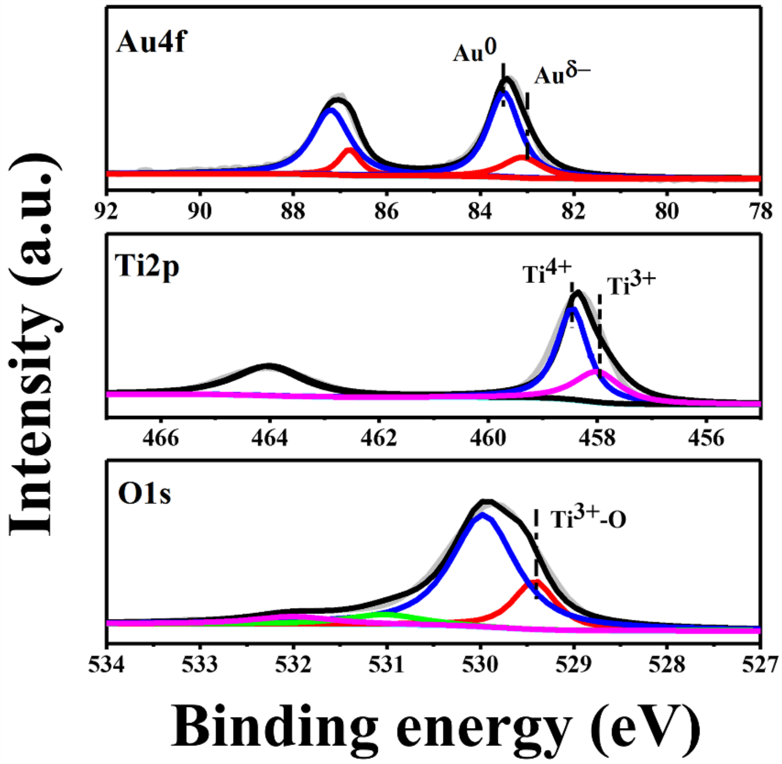

Figure S5. XPS spectra of Au 4*f*, Ti 2*p* and O 1*s* for Au/TiO_2(H300).

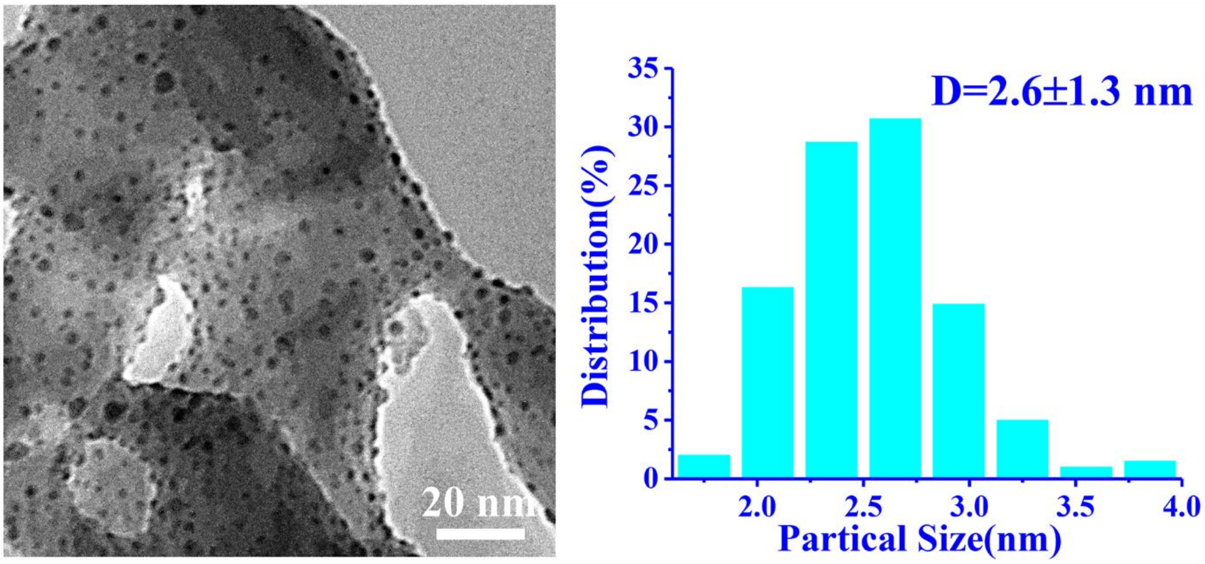

Figure S6. TEM image of 13.8 wt.% Au@TiO_{2-x}/ZnO(H300) and the corresponding size distribution of Au NPs. The size distribution was obtained by analyzing about 200 Au NPs from TEM image.

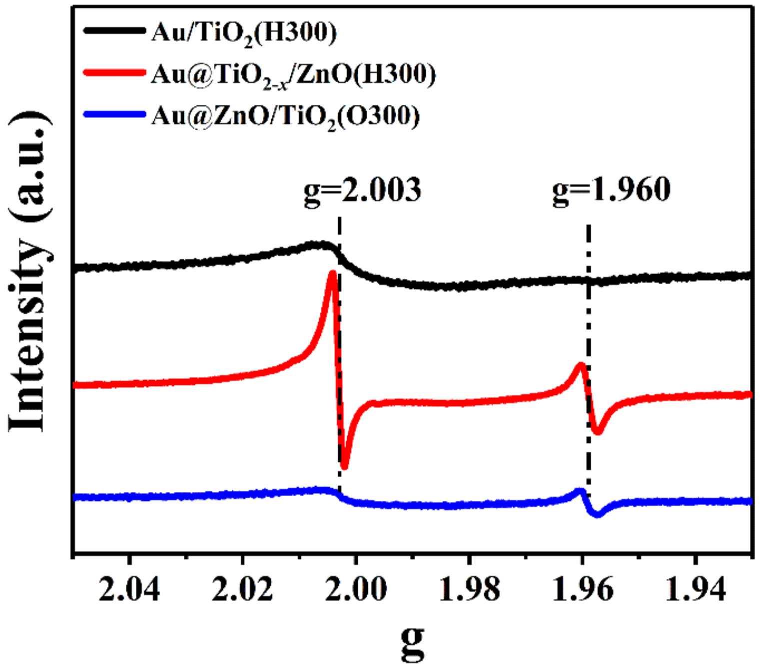

Figure S7. EPR spectra (obtained at 100 K) of Au/TiO_2(H300), Au@$TiO_{2\text{-}x}$/ZnO(H300) and Au@ZnO/TiO_2(O300), respectively.

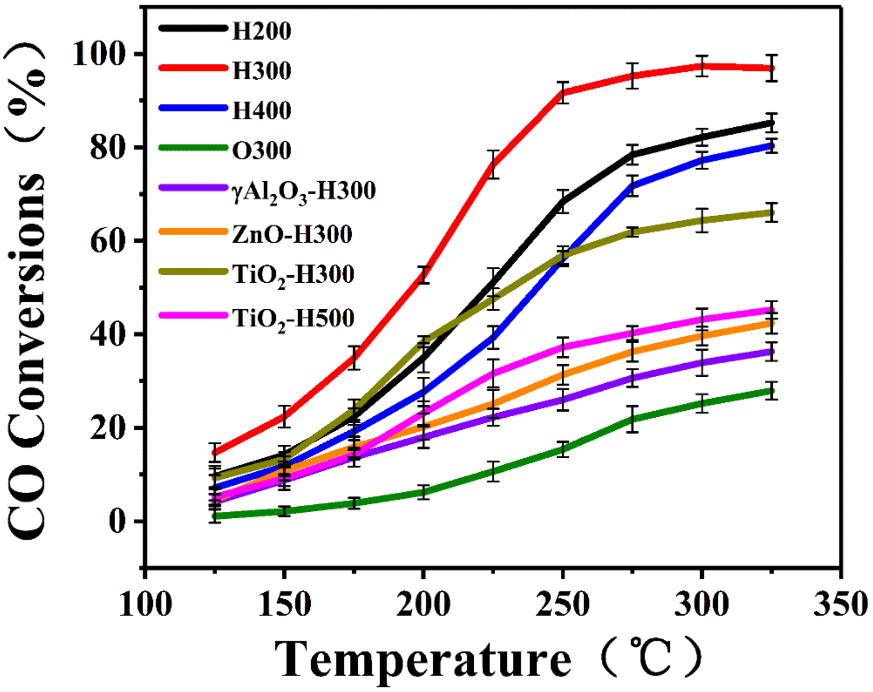

Figure S8. CO conversion as a function of reaction temperature over four Au/ZnTi-MMO samples and control samples: Au/ZnO(H300), Au/TiO_2(H300) and Au/γ-Al_2O_3(H300). WGS reaction conditions: 6% CO, 25% H_2O, 69% Ar; WHSV: 13200 mL g_{cat}^{-1} h^{-1}.

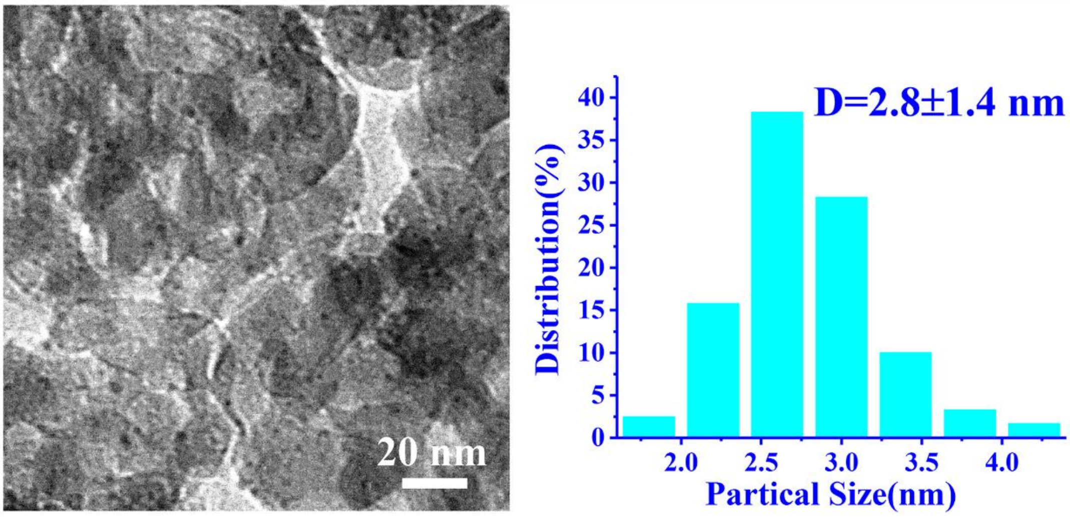

Figure S9. TEM image of Au/TiO$_2$(H300) and the corresponding size distribution of Au NPs. The size distribution was obtained by analyzing about 200 Au NPs from TEM image.

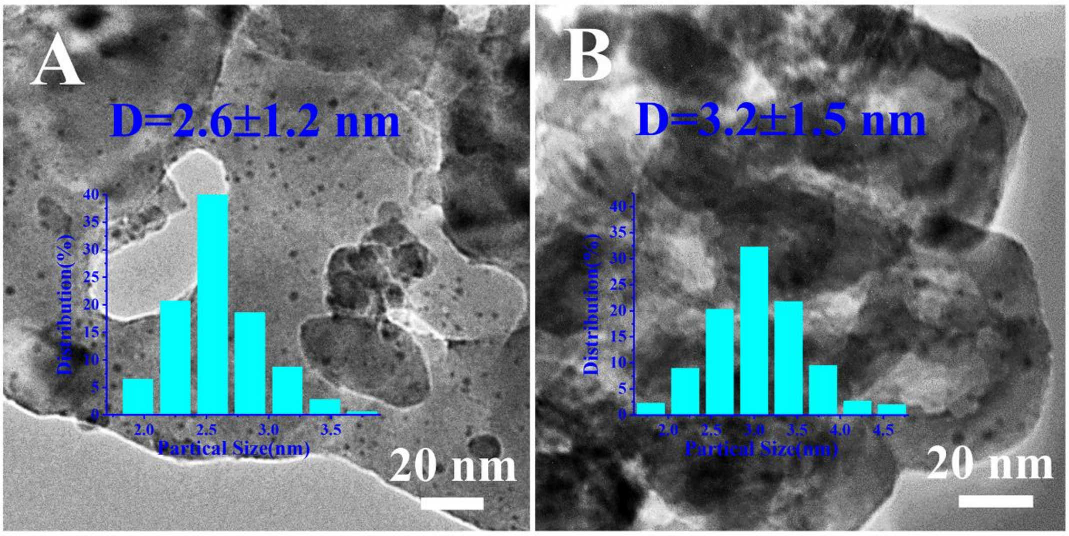

Figure S10. TEM images and the corresponding Au NPs size distribution of (A) Au@TiO$_{2-x}$/ZnO(H300) and (B) Au/TiO$_2$(H300) after 60 h stability test. The size distribution was obtained by analyzing about 200 Au NPs from TEM image.

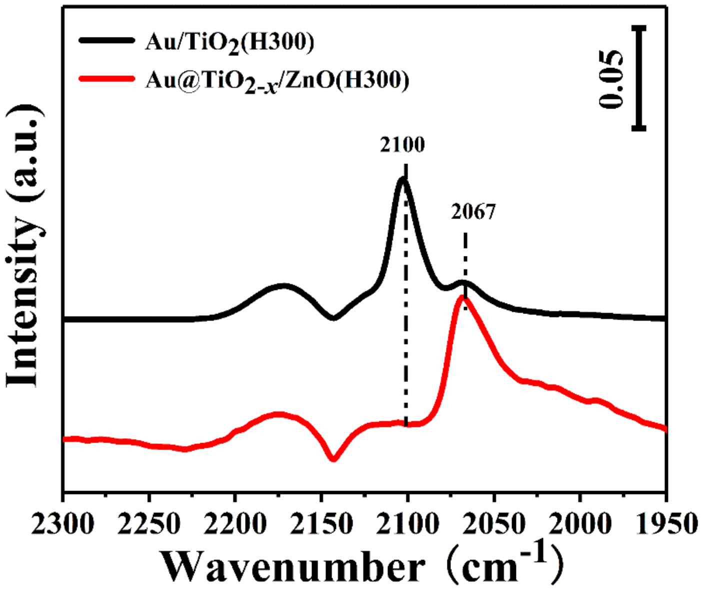

Figure S11. *In situ* DRIFT spectra of CO adsorption over Au/TiO_2(H300) and Au@TiO_{2-x}/ZnO(H300) at 25 ℃.

Table S1. Physicochemical properties of control samples

catalysts	BET surface area (m^2 g^{-1})	Content of Au species [a] (wt%)	Mean particle size of Au [b] (nm)	Theoretical dispersion of Au [c] (%)	Determined dispersion of Au [d] (%)	Surface content of Au species [e] (mmol g^{-1})	Coverage degree of Au [f] (%)
Au/TiO_2(H300)	64.3	1.9	2.8	41.3	28.7	0.028	30
Au/ZnO(H300)	58.6	1.8	–	–	–	–	–
Au/γ-Al_2O_3(H300)	89.5	1.9	–	–	–	–	–
15 wt % Au@TiO_{2-x}/ZnO(H300)	73.2	13.8	2.6	–	–	–	–

[a] Content of Au species was determined by inductively coupled plasma−atomic emission spectroscopy (ICP−AES). [b] Mean particle size of Au was determined by HRTEM. [c] Theoretical dispersion of Au was calculated based on the result of HRTEM. [d-e] Determined dispersion of Au and surface concentration of Au species were calculated based on the results of CO pulse chemisorption at 200 K. [f] Coverage degree of Au NPs was calculated based on the results of CO pulse chemisorption and Au particle size was measured by TEM.

Table S2. Surface elemental concentration derived from deconvolution results of XPS

Samples	Gold Species Percentage (%)		Titanium Species Percentage (%)	
	Au^0	$Au^{\delta-}$	Ti^{3+}	Ti^{4+}
Au@TiO_{2-x}/ZnO(H200)	39.7	60.3	41.1	58.9
Au@TiO_{2-x}/ZnO(H300)	30.3	69.7	71.9	28.1
Au@TiO_{2-x}/ZnO(H400)	49.2	50.8	29.1	70.9
Au@ZnO/TiO_2(O300)	100	0	15.1	84.9

Table S3. Comparison of catalytic performances toward WGSR over various gold-based catalysts

Catalysts	Au (wt. %)	Temp. (℃)	Gas Feed Composition	Reaction Rate [mol_{co} mol_{Au}^{-1} s^{-1}]	Ref.
Au@TiO_{2-x}/ZnO(H300)	2	250	6%CO-25%H_2O-Ar	0.15	This work
Au@TiO_{2-x}/ZnO(H300)	2	200	6%CO-25%H_2O-Ar	0.085	This work
Au@TiO_{2-x}/ZnO(H300)	2	150	6%CO-25%H_2O-Ar	0.039	This work
Au/ZnO(H300)	2	200	6%CO-25%H_2O-Ar	0.014	This work
Au/TiO_2(H300)	2	200	6%CO-25%H_2O-Ar	0.031	This work
Au/Al_2O_3(H300)	2	200	6%CO-25%H_2O-Ar	0.012	This work
Au/CeO_2	4.7	250	11%CO-26%H_2O-26%H_2-7%CO_2-He	0.13	1
Au/CeO_2	1	150	2%CO-10%H_2O-He	0.047	2
Au/CeO_x/TiO_2	2	227	1%CO-3%H_2O-He	0.031	3
Au/TiO_2	2.3	120	7%CO-11%-H_2O-9%CO_2-37%H_2	0.011	4
Au/TiO_2	4.87	200	11%CO-26%H_2O-26%H_2-7%CO_2-He	0.056	5
Au/CeFeAl	2.17	180	4.5%CO-30%H_2O-N_2	0.018	6
Au/CeFeAl	2.17	250	4.5%CO-30%H_2O-N_2	0.026	6
Au/Mo_2C	1.5	120	7%CO-22%H_2O-37%H_2-8.5%CO_2-Ar	0.021	7
Au/CeO_2	2.7	180	0.75%CO-3%H_2O-N_2	0.071	8

REFERENCES

(1) Fu, Q.; Saltsburg, H.; Flytzani-Stephanopoulos, M. Active Nonmetallic Au and Pt Species on Ceria-Based Water-Gas Shift Catalysts. *Science* **2003**, *301*, 935−938.

(2) Si, R.; Flytzani-Stephanopoulos, M. Shape and Crystal-Plane Effects of Nanoscale Ceria on the Activity of Au-CeO_2 Catalysts for the Water-Gas Shift Reaction. *Angew. Chem. Int. Ed.* **2008**, *47*, 2884−2887.

(3) Si, R.; Tao, J.; Evans, J.; Park, J. B.; Barrio, L.; Hanson, J. C.; Zhu, Y.; Hrbek, J.; Rodriguez, J. A. Effect of Ceria on Gold-Titania Catalysts for the Water-Gas Shift Reaction: Fundamental Studies for Au/CeO_x/TiO_2(110) and Au/CeO_x/TiO_2 Powders. *J. Phys. Chem. C* **2012**, *116*, 23547−23555.

(4) Wang, Jun.; Kispersky, V. F.; Delgass, W. N.; Ribeiro, F. H. Determination of the Au Active Site and Surface Active Species *via* Operando Transmission FTIR and Isotopic Transient Experiments on 2.3 wt.% Au/TiO_2 for the WGS Reaction. *J. Catal.* **2012**, *289*, 171−178.

(5) Yang, M.; Allard, L. F.; Flytzani-Stephanopoulos, M. Atomically Dispersed Au−$(OH)_x$ Species Bound on Titania Catalyze the Low-Temperature Water-Gas Shift Reaction. *J. Am. Chem. Soc*. **2013**, *135*, 3768−3771.

(6) Castano, M. G.; Reina, T. R.; Ivanova, S.; Centeno, M. A.; Odriozola, J. A. Pt vs. Au in Water-Gas Shift Reaction. *J. Catal.* **2014**, *314*, 1−9.

(7) Sabnis, K. D.; Cui, Y.; Akatay, M. C.; Shekhar, M.; Lee, W.; Miller, J. T.; Delgass, W. N.; Ribeiro, F. H. Water-Gas Shift Catalysis over Transition Metals Supported on Molybdenum Carbide. *J. Catal.* **2015**, *331*, 162−171.

(8) Abdel-Mageed, A. M.; Kučerová, G.; Bansmann, J.; R. Jürgen, B. R. Active Au Species During the Low-Temperature Water Gas Shift Reaction on Au/CeO_2: A Time-Resolved Operando XAS and DRIFTS Study. *ACS Catal.* **2017**, *7*, 6471−6484.